A Large-Bandgap Conjugated Polymer for Versatile Photovoltaic Applications with High Performance

Maojie Zhang, Xia Guo, Wei Ma, Harald Ade,* and Jianhui Hou**

Bulk heterojunction (BHJ) polymer solar cells (PSCs), where a blend film of conjugated polymers as the donors and fullerene derivatives as the acceptors acts as the active layer, have attracted considerable attention in both academia and industry because of their low cost, light weight, easy fabrication, and potential for use in flexible devices.[1–3] Over the past few years, rapid progress has been made in this field. Power conversion efficiencies (PCEs) of more than 10% for traditional single PSCs and 11% for tandem PSCs have been achieved.[4,5] This trend brightens the application future of PSCs.

As is well known, the PCE of a PSC is determined by three key factors: its open-circuit voltage (V_{oc}), short-circuit current (J_{sc}), and fill factor (FF).[6] These parameters are closely related to the optical and electrical properties of the polymers and the blend morphology of the active layer in BHJ PSCs. In particular, V_{oc} is directly determined by the energy gap between the highest occupied molecular orbital (HOMO) level of the electron donor (polymer) and the lowest unoccupied molecular orbital (LUMO) level of the acceptor (fullerene derivatives).[7] Hence, the donor–acceptor (D–A) alternating conjugated polymers attract much attention because of their tunable properties, including their optical absorption band, molecular energy level, and carrier mobility. Good photovoltaic performance with PCE over 10% has been obtained in PSCs based on D–A polymers.[4]

Over the past few years, introducing the fluorine atom to the acceptor unit of D–A conjugated polymer has become a promising method for enhancing the efficiency of PSCs.[8–14] The fluorination can simultaneously lower the LUMO and HOMO levels of the polymer while incurring only a minor effect on the optical bandgaps. Accordingly, BHJ PSCs based on these fluorinated copolymers exhibit higher V_{oc} and PCE than the corresponding non-fluorinated derivatives. However, this method is only used in several limited acceptor units that have suitable positions to attach fluorine atoms. Recently, our group successfully introduced the fluorine atoms to the conjugated side chain of the donor unit—benzodithiophene (BDT)—in D–A polymers.[15] It was found that when two fluorine atoms were introduced onto the conjugated side chains of BDT, the HOMO levels of the corresponding polymers decreased by 0.25 eV; hence, the V_{oc} of the PSCs improved by 0.18 V, and the J_{sc} and FF of the devices also increased to a certain extent. Consequently, the PCE increased by more than 30%. Therefore, fluorination on the donor unit of the D–A polymer can effectively tune the molecular energy levels of the polymers and improve the photovoltaic performance of the devices. Recently, rapid progresses have been made for conjugated polymer materials with large bandgaps and these polymers showed advantages in fabricating semitransparent PSCs[16] (ST-PSCs) and the PCEs of 4–5% for single junction devices have been achieved.[16b,c] Despite that the device performance is usually limited by the low J_{sc} due to the narrow absorption spectra of the polymers and thin thickness of active layer, there is still a large room for improving PCE of semitransparent PSCs. From the view of materials design, to tune the molecular energy levels of the polymer should be an effective way to improve the V_{oc} and hence PCE of the device. As mentioned above, introducing the BDT unit with fluorine substituent (BDT-F) units to the backbone of large-bandgap polymers may be a good way to improve the photovoltaic performance.

Herein, we synthesized a new copolymer **PM6** based on 4,8-bis(5-(2-ethylhexyl)-4-fluorothiophen-2-yl)benzo[1,2-*b*:4,5-*b*′]-dithiophene (BDT-F) and 1,3-bis(thiophen-2-yl)-5,7-bis(2-ethylhexyl)benzo-[1,2-*c*:4,5-*c*′]dithiophene-4,8-dione (BDD), as shown in **Scheme 1**a. The optical, electrochemical, and photovoltaic properties, the molecular packing pattern, and the morphology of the blend films were investigated. Compared with the non-fluorinated derivative **PBDTBDD** in Scheme 1a, **PM6** exhibited a similar optical bandgap of ≈1.80 eV and a deeper HOMO level of -5.45 eV (–5.25 eV for **PBDTBDD**[17], which is beneficial for a high V_{oc}. BHJ PSCs based on **PM6**/PC_{71} BM with both conventional and inverted device structures were fabricated and showed promising photovoltaic performance: a high V_{oc} of 0.98 V and a PCE of 8% for the conventional devices and up to 9.2% for the inverted devices. Furthermore, the **PM6**/PC_{71} BM-based semitransparent device exhibited a PCE of 5.7%, which is among the highest values obtained for a semitransparent single-junction device. In addition, we found that the neat film of **PM6** exhibited strong crystallinity and a dominant face on

Prof. M. Zhang, Dr. X. Guo, Prof. J. Hou
State Key Laboratory of Polymer
Physics and Chemistry
Institute of Chemistry
Chinese Academy of Sciences
Beijing 100190, China
E-mail: hjhzlz@iccas.ac.cn
Prof. M. Zhang, Dr. X. Guo
Laboratory of Advanced Optoelectronic Materials
College of Chemistry
Chemical Engineering and Materials Science
Soochow University
Suzhou 215123, China
Prof. W. Ma
State Key Laboratory for Mechanical Behavior of Materials
Xi'an Jiaotong University
Xi'an 710049, P. R. China
E-mail: msewma@mail.xjtu.edu.cn
Prof. W. Ma, Prof. H. Ade
Department of Physics
North Carolina State University
Raleigh, NC 27695, USA
E-mail: hwade@ncsu.edu

DOI: 10.1002/adma.201502110

ADVANCED MATERIALS
www.advmat.de

www.MaterialsViews.com

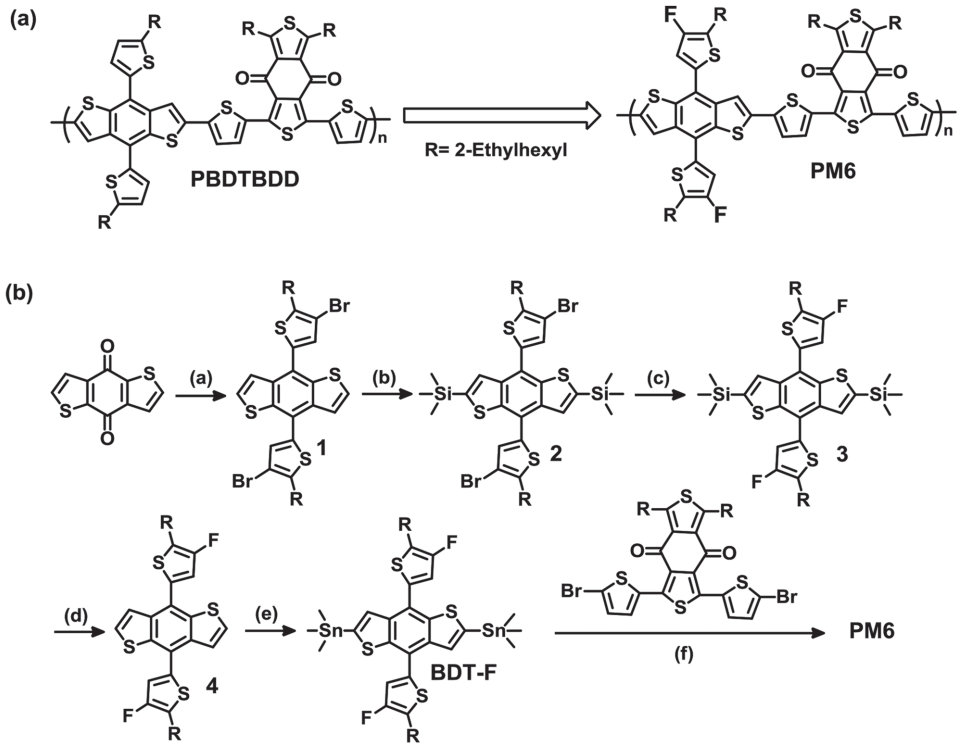

Scheme 1. a) Molecular structures of **PBDTBDD** and **PM6** and b) synthetic routes for the monomer BDT-F and **PM6**: (a) 3-bromo-2-(2-ethylhexyl)-thiophene, THF, LDA, –78 °C, 1 h; benzo[1,2-*b*:4,5-*b'*]dithiophen-4,8-dione, 50 °C, 2 h; then, $SnCl_2{\cdot}2H_2O$, HCl, 50 °C, overnight. (b) LDA, –78 °C, 1 h; Si$(CH_3)_3Cl$, rt, 2 h. (c) *n*-BuLi, THF, –78 °C; $PhSO_2NF$, rt, overnight. (d) $CF_3COOH/CHCl_3$, room temperature, 5 h. (e) LDA, THF, –78 °C, 1 h; Sn$(CH_3)_3Cl$, room temperature, 2 h. (f) Pd $(PPh_3)_4$, toluene/DMF, 110 °C.

packing with respect to the electrodes, which is advantageous for charge transport. These results indicate that **PM6** is a promising material for photovoltaic application.

The synthetic routes of the monomer (BDT-F) and **PM6** are shown in Scheme 1b. The monomer BDT-F was synthesized according to our previously reported procedures.[15] **PM6** was synthesized using a Pd-catalyzed Stille-coupling reaction. The polymer exhibits good solubility in chlorinated solvents such as chloroform, chlorobenzene, and *o*-dichlorobenzene (*o*-DCB). The number average molecular weight (M_n) and polydispersity index (PDI) of the polymer are 19.3 K and 2, respectively, which were estimated using gel-permeation chromatography (GPC) with 1,2,4-tricholorobenzene as the solvent and polystyrene as a standard.

As shown in **Figure 1**a, the UV–vis absorption spectra of **PM6** in the solution show two distinct absorption bands in the range of 300–700 nm, which is typically observed for D–A copolymers. The absorption maximum of **PM6** is located at ≈550 nm in the solution. In the solid film, the absorption maximum is redshifted to 570 nm, and a strong shoulder peak at ≈614 nm is observed, which should be attributed to the strong aggregation of polymer chains in the solid state. The absorption edge (λ_{edge}) of the polymer film is at ≈690 nm, which corresponds to an optical bandgap (E_g^{opt}) of ≈1.80 eV. Electrochemical cyclic voltammetry (CV) was performed to determine the HOMO level of the polymer. As shown in Figure 1b, the onset oxidation potential (ϕ_{ox}) is 0.74 V versus Ag/Ag^+, which corresponds to a HOMO level of –5.45 eV. This

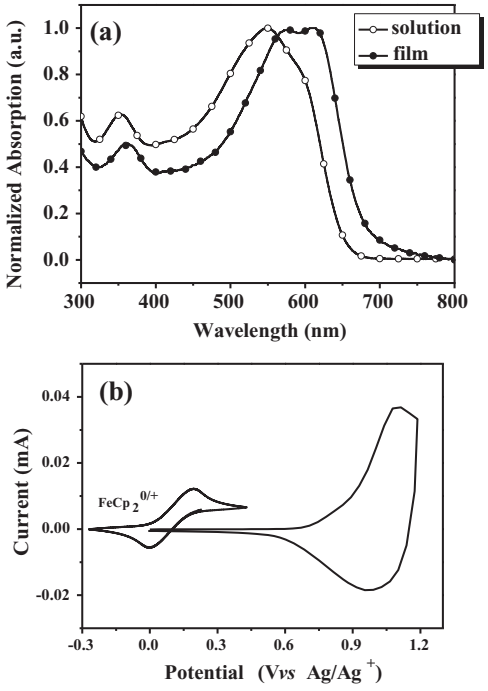

Figure 1. a) Absorption spectra of **PM6** in chloroform and film and b) cyclic voltammogram of the polymer film on a platinum electrode, which was measured in 0.1 mol L^{-1} Bu_4NPF_6 acetonitrile solutions at a scan rate of 50 mV s^{-1}.

DOI: 10.1002/adma.201502110

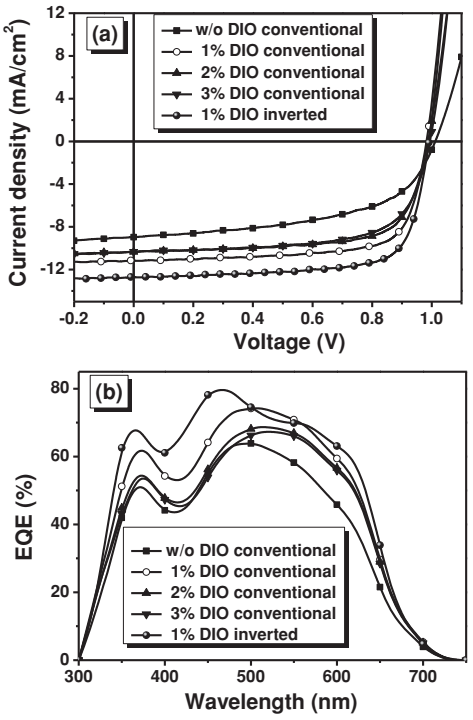

Figure 2. a) *J–V* characteristics and b) EQE curves of solar cells based on the **PM6**/$PC_{71}BM$ (1:1.2, w/w) blend with different additive contents.

HOMO level was calculated using the following equation: HOMO = $-e(\phi_{ox} + 4.71)$ (eV).[18] **PM6** exhibits a relatively low LUMO level of −3.65 eV, which was calculated from the HOMO level and optical bandgap. Compared with the non-fluorinated derivative **PBDTBDD**, the HOMO level of **PM6** decreased by 0.22 eV because two fluorine atoms were introduced at the BDT side chains, which was beneficial for the high V_{oc} in polymer solar cells. Moreover, the LUMO and HOMO energy levels of **PBDTBDD** and **PM6** were calculated by density functional theory (DFT) (B3LYP/6-31G (d, p)) as shown in Figure S1 (Supporting Information). The results indicated that attaching fluorine atoms to the BDT side chains could reduce both HOMO and LUMO levels of the polymer simultaneously.

Conventional BHJ PSC devices with the configuration of ITO/poly(3,4-ethylenedioxythiophene):polystyrenesulfonic acid (PEDOT:PSS)/**PM6**:$PC_{71}BM$/Ca/Al were fabricated with *o*-DCB as the solvent and were tested under the illumination of AM 1.5G (100 mW cm^{-2}). The D/A weight ratios (**PM6**/$PC_{71}BM$, w/w) of the blend in the active layer were optimized (Figure S2 and Table S1, Supporting Information). It was found that the optimal D/A weight ratio of the blend was 1:1.2, and a PCE of 5.3% was obtained with V_{oc} = 1.02 V, J_{sc} = 9.3 mA cm^{-2}, and FF = 56%. **Figure 2** shows the current-density–voltage (*J–V*) characteristics and external quantum efficiency (EQE) curves of the solar cells based on the **PM6**/$PC_{71}BM$ (1:1.2, w/w) blend spin-coated without additive and with 1%, 2%, and 3% 1,8-diiodooctane (DIO/*o*-DCB, v/v). The photovoltaic parameters of the fabricated devices under optimal conditions are summarized in **Table 1**. Compared with the devices that were processed without additive, the devices that were processed with DIO showed higher J_{sc} and FF; thus, PCE was enhanced, despite

Table 1. Photovoltaic properties of the PSCs based on **PM6** and $PC_{71}BM$ (1:1.2, w/w) under the illumination of AM 1.5G, 100 mW cm^{-2}.

DIO [v/v%]	V_{oc} [V]	J_{sc} [mA cm^{-2}]	FF [%]	PCE_{max} (PCE_{ave}[a]) [%]	Thickness [nm]
–	1.02	9.3	56	5.3 (5.1)	78
1	0.98	11.2	73	8 (7.8)	75
1[b]	0.98	12.7	74	9.2 (8.8)	75
1[c]	0.96	9.4	63	5.7 (5.4)	75
2	0.98	10.4	70	7.1 (6.9)	75
3	0.98	10.3	67	6.8 (6.6)	75

[a]The average PCE was obtained from more than 20 devices; [b]Inverted structure of ITO/PFN/PM6:$PC_{71}BM$/MoO_3/Au (80 nm); [c]Semitransparent device with the structure of ITO/PFN/PM6:$PC_{71}BM$/MoO_3/Au (10 nm).

the slightly lower V_{oc}. The best performance was obtained when 1% DIO was used, and a maximum PCE = 8% was found with V_{oc} = 0.98 V, J_{sc} = 11.2 mA cm^{-2}, and FF = 73%. As shown in Figure 2b, EQE was obviously enhanced for the solar cells that were fabricated with DIO as the additive. When 1% DIO was added, the quantum efficiency of the device significantly increased in the wavelength range of 350–650 nm, and a maximum EQE of 74% at 510 nm was recorded. The integrated J_{sc} values from the EQE curves are consistent with the observed J_{sc} values in the *J–V* measurement, and the deviation is within 5%. To further improve the photovoltaic performance, an inverted device with the structure of ITO/poly [(9,9-bis(3′-(*N*,*N*-dimethylamino)propyl)-2,7-fluorene)-*alt*-2,7-(9,9-dioctylfluorene) (PFN)/**PM6**:$PC_{71}BM$/MoO_3/Au was fabricated. Compared with the conventional device, the inverted device exhibited higher J_{sc} of 12.7 mA cm^{-2}, which resulted from the better charge collection and transmission of PFN than PEDOT:PSS.[19] Consequently, the high PCE of 9.2% was achieved for the inverted devices.

Semitransparent solar cells have great potential to be used in many photovoltaic applications, such as building-integrated photovoltaics and solar windows.[16] Considering the **PM6**/$PC_{71}BM$-based device performed well when the thin film was only ≈75 nm, it would be a potential material for semitransparent PSC application. Therefore, the ST-PSCs were fabricated with the structure of ITO/PFN/**PM6**:$PC_{71}BM$/MoO_3/Au (10 nm). **Figure 3** shows the transmission spectrum and *J–V* curves of the semitransparent PSC. The average light transmission in the visible range of 380–780 nm reaches ≈67%, and the maximum approaches 100% at the wavelength of 701 nm. In the photograph of the device, the flowers and leaves are clearly observed. The device also exhibited a PCE of 5.7% with V_{oc} = 0.96 V, J_{sc} = 9.4 mA cm^{-2}, and FF = 63% under the illumination of AM 1.5G, 100 mA cm^{-2}, which is among the highest values for single-junction ST-PSCs. These results indicate that **PM6** is a promising material for versatile photovoltaic applications.

Grazing-incidence X-ray diffraction (GIXD) and resonant soft X-ray scattering (RSoXS) were used to investigate the effect of the additive on the morphology of the blend films. **Figure 4**a shows the in-plane (IP) and out-of-plane (OOP) GIXD profiles of the samples, including the thin films of the pure **PM6** film and **PM6**:$PC_{71}BM$ blend (1:1, w/w) films, which were cast from *o*-DCB without or with DIO as a processing additive. For the

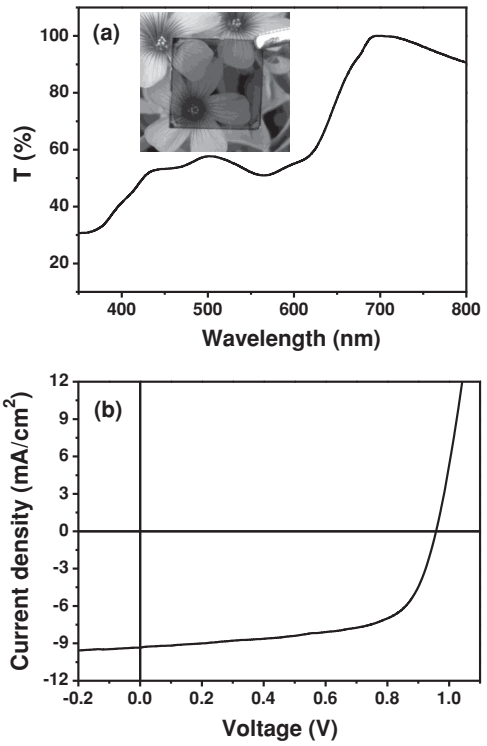

Figure 3. a) Transmission spectrum and photograph of the semitransparent device and b) current-density–voltage characterization of the semitransparent polymer solar cell with the device structure of ITO/PFN/**PM6**:$PC_{71}BM$/MoO_3/Au.

neat polymer film, the OOP profile shows pronounced (100) diffraction peaks at 0.31 Å^{-1} with a *d*-spacing of 20.3 Å, whereas the IP profile also exhibits strong (100) and weak (200) diffraction peaks at 0.31 and 0.62 Å^{-1}, respectively. In addition, the OOP profile shows one sharp and intensive peak at 1.66 Å^{-1}, which corresponds to the (010) π–π stacking with a *d*-spacing of ≈3.78 Å. This result implies that the neat polymer film exhibits a face-on dominated molecular orientation with respect to the substrate. When blended with $PC_{71}BM$, the IP (100) peak was distinctly weakened, whereas the OOP (100) peak hardly changed. Meanwhile, the π–π stacking of the polymer in the blend films was completely disrupted. The broad peak at $q \approx 1.4$ Å^{-1} is attributed to $PC_{71}BM$ aggregation. When DIO was used as an additive, the lamellar diffraction and π–π stacking diffraction significantly increased; with an increasing amount of DIO, the lamellar stacking continued increasing, and the π–π stacking remained almost unchanged. We also calculated the coherence length (L_{100}), which was deduced from the full width at half maximum (FWHM) of IP (100) peaks using Sherrer equation.[20] The values of 1.1, 1.4, and 2.2 nm for 1%, 2%, and 3% DIO were obtained, which are substantially increased with increasing DIO contents from 1% to 3%. Hence, with DIO as an additive, the overall crystallinity of the polymer was enhanced.

The phase-separated morphologies of the blends prepared using different conditions were further investigated using RSoXS.[21,22] A photon energy of 284.2 eV was selected to provide high polymer/fullerene contrast while avoiding the high absorption associated with the carbon 1s core level, which

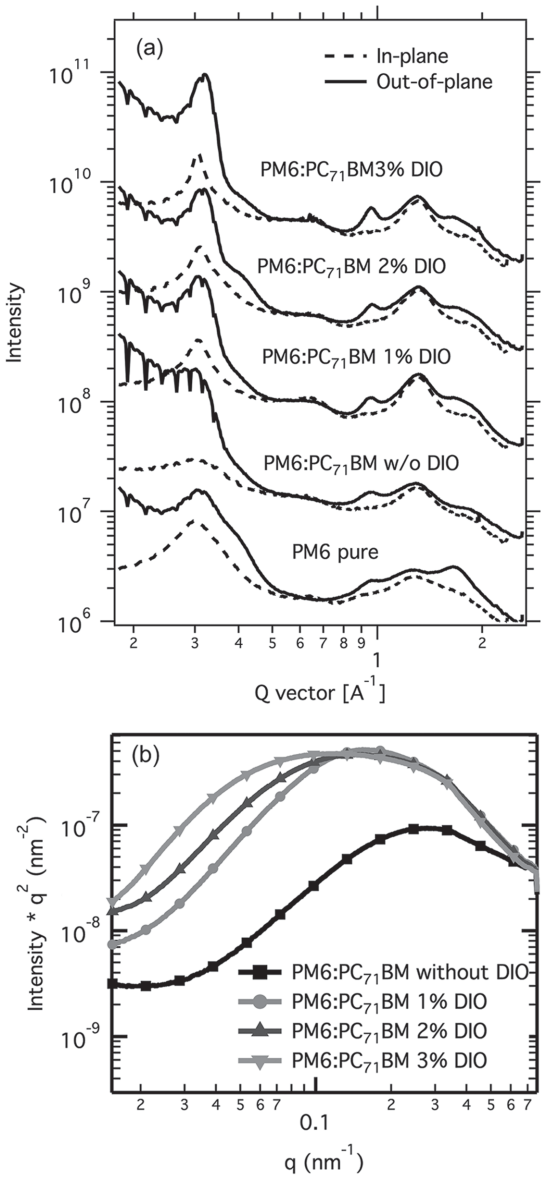

Figure 4. a) GIXD profiles for the pure film of **PM6** and blend films of **PM6**:$PC_{71}BM$ (1:1.2, w/w) with different amounts of DIO and b) RSoXS profiles for the blend films of **PM6**:$PC_{71}BM$ (1:1.2, w/w) with different amounts of DIO.

would produce background fluorescence and could lead to radiation damage.[23] Figure 4b shows the RSoXS profiles of the polymer:$PC_{71}BM$ (1:1.2, w/w) blend films that were cast from the *o*-DCB without or with DIO as a processing additive. The scattering profiles represent the distribution function of spatial frequency *s* ($s = q/2\pi$) of the samples and are dominated by log-normal distributions, which can be fitted by a set of Gaussians in the lin-log space. The distribution median s_{median} corresponds to the characteristic median length scale ξ of the corresponding log-normal distribution in real space with $\xi = 1/s_{median}$, which is a model-independent statistical quantity. When the blend films were processed with pure *o*-DCB, the profile showed a low scattering intensity with ξ of ≈20 nm, which indicates that

Adv. Mater. **2015**,
DOI: 10.1002/adma.201502110

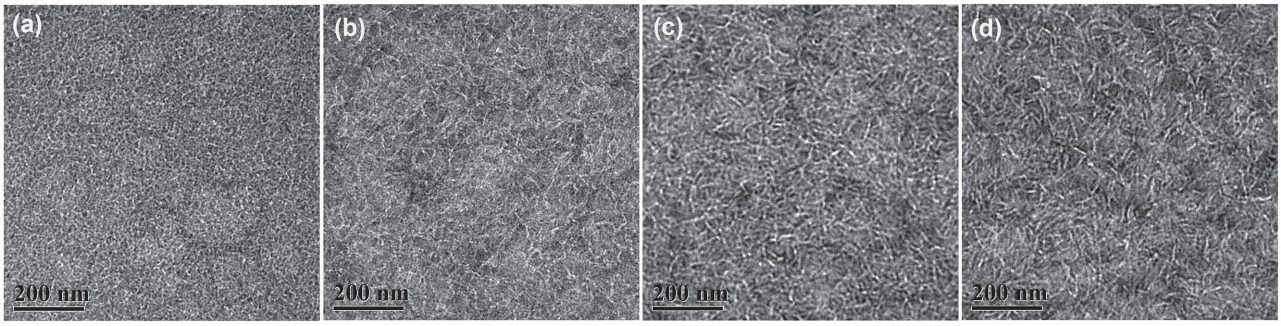

Figure 5. TEM images of PM6:$PC_{71}BM$ blend films: a) without DIO; b) with 1% DIO; c) with 2% DIO; and d) with 3% DIO.

the phase separation is weak and resulted in notably impure domains. When DIO was used as the additive, the scattering profile showed a much higher intensity and two log-normal distributions (Figure S3, Supporting Information). At high q, the value of ξ is located at ≈20 nm irrespective of processing, but at low q, ξ increases with the increase in DIO concentration. The corresponding ξ increases, i.e., 40, 45, and 63 nm for 1%, 2%, and 3% DIO, respectively. It is evident that the films that were cast with DIO as the additive show hierarchical or a two-length-scale structure and exhibit phase separation at a small length scale that is similar to that of the blend film that was processed using pure *o*-DCB. It is reported that the hierarchical structure is a favorable morphology to improve the device performance.[24,25] Similarly, sufficient aggregation of the polymer and fullerene has to be present. Here, the improved performance is consistent with this paradigm and occurs due to the creation of more pure domain that provide better charge transport and reduced recombination. As the domains get too large, exciton harvesting suffers.

Furthermore, the surface and bulk of the blend films were also studied using atomic force microscopy (AFM) and transmission electron microscopy (TEM). As shown in Figure S4 (Supporting Information), the root-mean-square (RMS) values are 0.61, 1.63, 2.03, and 2.27 nm for the blends processed without additive and with 1% DIO, 2% DIO, and 3% DIO, respectively. However, increasing the amount of DIO results in an enhanced phase separation, which should be caused by the enhanced polymer crystallinity. As shown in **Figure 5**, the blend film that was processed using only *o*-DCB shows a poor phase separation. When 1% DIO was added as the additive, a fibrillar network was clearly observed. When more DIO was added, the phase separation became much stronger, and the mesh size between the fibrils became larger. As previously mentioned, the AFM and TEM results are consistent with the GIXD and RSoXS measurements.

In summary, a new copolymer based on BDT-F as the donor and BDD as the acceptor, which is named **PM6**, was designed and synthesized for photovoltaic applications. The polymer exhibited a large bandgap of 1.80 eV and a deep HOMO energy level of −5.45 eV. The **PM6**-based inverted PSCs showed high PCE of 9.2% and V_{oc} of 0.98 V with a relatively thin film thickness of 75 nm, which is beneficial for tandem PSCs. Furthermore, the **PM6**-based semitransparent device exhibited a high average transmission of 67% in the visible range and a PCE of 5.6%, which is among the high values for single-junction semitransparent PSCs. These results indicate that **PM6** is a versatile material for opaque or semitransparent single-junction PSCs and tandem PSCs.

Supporting Information

Supporting Information is available from the Wiley Online Library or from the author.

Acknowledgements

The authors would like to acknowledge the financial support from the Natural Science Foundation of China (Nos. 20874106, 21325419, 51203168, 51422306, and 91333204). The X-ray characterization by M.W. and H.A. was supported by the U.S. Department of Energy, Office of Science, Basic Energy Science, Division of Materials Science and Engineering under Contract No. DE-FG02-98ER45737. The X-ray data were acquired at beamlines 11.0.1.2[26] and 7.3.3[27] at the Advanced Light Source, which was supported by the Director, Office of Science, Office of Basic Energy Sciences of the U.S. Department of Energy under Contract No. DE-AC02-05CH11231.

Received: May 2, 2015
Revised: June 10, 2015
Published online:

[1] a) J. W. Chen, Y. Cao, *Acc. Chem. Res.* **2009**, *42*, 1709; b) G. Li, R. Zhu, Y. Yang, *Nat. Photonics* **2012**, *6*, 153; c) Y. F. Li, *Acc. Chem. Res.* **2012**, *45*, 723; d) I. Mcculloch, R. S. Ashraf, L. Biniek, H. Bronstein, C. Combe, J. E. Donaghey, D. I. James, C. B. Nielsen, B. C. Schroeder, W. M. Zhang, *Acc. Chem. Res.* **2012**, *45*, 714.

[2] a) K. Müllen, T. M. Swager, *Acc. Chem. Res.* **2008**, *41*, 1085; b) B. C. Thompson, J. M. J. Fréchet, *Angew. Chem. Int. Ed.* **2008**, *47*, 58.

[3] a) Y. J. Cheng, S. H. Yang, C. S. Hsu, *Chem. Rev.* **2009**, *109*, 5868; b) G. Dennler, M. C. Scharber, C. J. Brabec, *Adv. Mater.* **2009**, *21*, 1323; c) L. Ye, S. Q. Zhang, L. J. Huo, M. J. Zhang, J. H. Hou, *Acc. Chem. Res.* **2014**, *47*, 1595.

[4] a)J. D. Chen, C. Cui, Y. Q. Li, L. Zhou, Q. D. Ou, C. Li, Y. Li, J. X. Tang, *Adv. Mater.* **2015**; *27* 1035 b) Y. Liu, J. Zhao, Z. Li, C. Mu, W. Ma, H. Hu, K. Jiang, H. Lin, H. Ade, H. Yan, *Nat. Commun.* **2014**, *5*, 5293; c) S. Q. Zhang, L. Ye, W. C. Zhao, B. Yang, Q. Wang, J. H. Hou, *Sci. China, Ser. B: Chem.* **2015**, *58*, 248.

[5] a) L. T. Dou, J. B. You, J. Yang, C. C. Chen, Y. J. He, S. Murase, T. Moriarty, K. Emery, G. Li, Y. Yang, *Nat. Photonics* **2012**, *6*, 180; b) C. C. Chen, W. H. Chang, K. Yoshimura, K. Ohya, J. You, J. Gao,

Z. Hong, Y. Yang, *Adv. Mater.* **2014**, *26*, 5670; c) Z. Zheng, S. Zhang, M. Zhang, K. Zhao, L. Ye, Y. Chen, B. Yang, J. Hou, *Adv. Mater.* **2015**, *27*, 1189; d) J. H. Kim, J. B. Park, F. Xu, D. Kim, J. Kwak, A. C. Grimsdale, D. H. Hwang, *Energy Environ. Sci.* **2014**, *7*, 4118.

[6] a) P. M. Beaujuge, J. M. J. Fréchet, *J. Am. Chem. Soc.* **2011**, *133*, 20009; b) M. J. Zhang, X. Guo, Y. F. Li, *Adv. Energy Mater.* **2011**, *1*, 557; c) X. Guo, C. H. Cui, M. J. Zhang, L. J. Huo, Y. Huang, J. H. Hou, Y. Li, *Energy Environ. Sci.* **2012**, *5*, 7943; d) Z. B. Henson, K. Müllen, G. C. Bazan, *Nat. Chem.* **2012**, *4*, 699; e) R. A. Janssen, J. Nelson, *Adv. Mater.* **2013**, *25*, 1847.

[7] a) P. W. M. Blom, V. D. Mihailetchi, L. J. A. Koster, D. E. Markov, *Adv. Mater.* **2007**, *19*, 1551; b) C. J. Brabec, S. Gowrisanker, J. J. M. Halls, D. Laird, S. J. Jia, S. P. Williams, *Adv. Mater.* **2010**, *22*, 3839.

[8] a) Y. Y. Liang, D. Q. Feng, Y. Wu, S. T. Tsai, G. Li, C. Ray, L. P. Yu, *J. Am. Chem. Soc.* **2009**, *131*, 7792; b) H. J. Son, W. Wang, T. Xu, Y. Y. Liang, Y. E. Wu, G. Li, L. P. Yu, *J. Am. Chem. Soc.* **2011**, *133*, 1885.

[9] a) Z. Li, J. P. Lu, S. C. Tse, J. Y. Zhou, X. M. Du, Y. Tao, J. F. Ding, *J. Mater. Chem.* **2011**, *21*, 3226; b) S. C. Price, A. C. Stuart, L. Q. Yang, H. X. Zhou, W. You, *J. Am. Chem. Soc.* **2011**, *133*, 4625; c) Y. Zhang, S. C. Chien, K. S. Chen, H. L. Yip, Y. Sun, J. A. Davies, F. C. Chen, A. K. Y. Jen, *Chem. Commun.* **2011**, *47*, 11026; d) H. X. Zhou, L. Q. Yang, A. C. Stuart, S. C. Price, S. B. Liu, W. You, *Angew. Chem. Int. Ed.* **2011**, *50*, 2995; e) H. C. Chen, Y. H. Chen, C. C. Liu, Y. C. Chien, S. W. Chou, P. T. Chou, *Chem. Mater.* **2012**, *24*, 4766.

[10] a) J. F. Jheng, Y. Y. Lai, J. S. Wu, Y. H. Chao, C. L. Wang, C. S. Hsu, *Adv. Mater.* **2013**, *25*, 2445; b) A. C. Stuart, J. R. Tumbleston, H. X. Zhou, W. T. Li, S. B. Liu, H. Ade, W. You, *J. Am. Chem. Soc.* **2013**, *135*, 1806; c) L. Q. Yang, J. R. Tumbleston, H. X. Zhou, H. Ade, W. You, *Energy Environ. Sci.* **2013**, *6*, 316.

[11] a) S. Albrecht, S. Janietz, W. Schindler, J. Frisch, J. Kurpiers, J. Kniepert, S. Inal, P. Pingel, K. Fostiropoulos, N. Koch, D. Neher, *J. Am. Chem. Soc.* **2012**, *134*, 14932; b) Y. Zhang, J. Y. Zou, C. C. Cheuh, H. L. Yip, A. K. Y. Jen, *Macromolecules* **2012**, *45*, 5427; c) H. Bronstein, J. M. Frost, A. Hadipour, Y. Kim, C. B. Nielsen, R. S. Ashraf, B. P. Rand, S. Watkins, I. McCulloch, *Chem. Mater.* **2013**, *25*, 277.

[12] a) J. W. Jo, J. W. Jung, H.-W. Wang, P. Kim, T. P. Russell, W. H. Jo, *Chem. Mater.* **2014**, *26*, 4214; b) Q. Peng, X. J. Liu, D. Su, G. W. Fu, J. Xu, L. M. Dai, *Adv. Mater.* **2011**, *23*, 4554; c) Y. C. Yang, R. M. Wu, X. Wang, X. P. Xu, Z. J. Li, K. Li, Q. Peng, *Chem. Commun.* **2014**, *50*, 439; d) K. Li, Z. J. Li, K. Feng, X. P. Xu, L. Y. Wang, Q. Peng, *J. Am. Chem. Soc.* **2013**, *135*, 13549.

[13] a) W. Li, S. Albrecht, L. Yang, S. Roland, J. R. Tumbleston, T. McAfee, L. Yan, M. A. Kelly, H. Ade, D. Neher, W. You, *J. Am. Chem. Soc.* **2014**, *136*, 15566; b) W. Li, L. Yang, J. R. Tumbleston, L. Yan, H. Ade, W. You, *Adv. Mater.* **2014**, *26*, 4456.

[14] a) P. Liu, K. Zhang, F. Liu, Y. Jin, S. Liu, T. P. Russell, H.-L. Yip, F. Huang, Y. Cao, *Chem. Mater.* **2014**, *26*, 3009; b) T. L. Nguyen, H. Choi, S. J. Ko, M. A. Uddin, B. Walker, S. Yum, J. E. Jeong, M. H. Yun, T. J. Shin, S. Hwang, J. Y. Kim, H. Y. Woo, *Energy Environ. Sci.* **2014**, *7*, 3040.

[15] M. J. Zhang, X. Guo, S. Q. Zhang, J. H. Hou, *Adv. Mater.* **2014**, *26*, 1118.

[16] a) K.-S. Chen, J.-F. Salinas, H.-L. Yip, L. Huo, J. Hou, A. K. Y. Jen, *Energy Environ. Sci.* **2012**, *5*, 9551; b) Z. M. Beiley, M. G. Christoforo, P. Gratia, A. R. Bowring, P. Eberspacher, G. Y. Margulis, C. Cabanetos, P. M. Beaujuge, A. Salleo, M. D. McGehee, *Adv. Mater.* **2013**, *25*, 7020; c) C.-Y. Chang, L. Zuo, H.-L. Yip, Y. Li, C.-Z. Li, C.-S. Hsu, Y.-J. Cheng, H. Chen, A. K. Y. Jen, *Adv. Funct. Mater.* **2013**, *23*, 5084; d) C.-Y. Chang, L. Zuo, H.-L. Yip, C.-Z. Li, Y. Li, C.-S. Hsu, Y.-J. Cheng, H. Chen, A. K. Y. Jen, *Adv. Energy Mater.* **2014**, *4*, 1301645; e)A. R. B. M. Yusoff, S. J. Lee, F. K. Shneider, W. J. da Silva, J. Jang, *Adv. Energy Mater.* **2014**, *4*, 1301989.

[17] D. P. Qian, L. Ye, M. J. Zhang, Y. R. Liang, L. J. Li, Y. Huang, X. Guo, S. Q. Zhang, Z. A. Tan, J. H. Hou, *Macromolecules* **2012**, *45*, 9611.

[18] a) M. J. Zhang, H. J. Fan, X. Guo, Y. J. He, Z. G. Zhang, J. Min, J. Zhang, G. J. Zhao, X. W. Zhan, Y. F. Li, *Macromolecules* **2010**, *43*, 5706; b) X. Guo, M. J. Zhang, J. H. Tan, S. Q. Zhang, L. J. Huo, W. P. Hu, Y. F. Li, J. H. Hou, *Adv. Mater.* **2012**, *24*, 6536.

[19] a) Z. C. He, C. M. Zhong, X. Huang, W. Y. Wong, H. B. Wu, L. W. Chen, S. J. Su, Y. Cao, *Adv. Mater.* **2011**, *23*, 4636; b) Z. C. He, C. M. Zhong, S. J. Su, M. Xu, H. B. Wu, Y. Cao, *Nat. Photonics* **2012**, *6*, 591; c) X. Hu, C. Yi, M. Wang, C.-H. Hsu, S. Liu, K. Zhang, C. Zhong, F. Huang, X. Gong, Y. Cao, *Adv. Energy Mater.* **2014**, *4*, 1400378.

[20] S.-J. Ko, W. Lee, H. Choi, B. Walker, S. Yum, S. Kim, T. J. Shin, H. Y. Woo, J. Y. Kim, *Adv. Energy Mater.* **2015**, DOI:10.1002/aenm.201401687.

[21] a) M. J. Zhang, Y. Gu, X. Guo, F. Liu, S. Q. Zhang, L. J. Huo, T. P. Russell, J. H. Hou, *Adv. Mater.* **2013**, *25*, 4944; b) X. Guo, M. J. Zhang, W. Ma, L. Ye, S. Q. Zhang, S. J. Liu, H. Ade, F. Huang, J. H. Hou, *Adv. Mater.* **2014**, *26*, 4043; c) W. Ma, J. R. Tumbleston, L. Ye, C. Wang, J. H. Hou, H. Ade, *Adv. Mater.* **2014**, *26*, 4234; d) M. J. Zhang, X. Guo, W. Ma, H. Ade, J. H. Hou, *Adv. Mater.* **2014**, *26*, 5880.

[22] a) S. Swaraj, C. Wang, H. P. Yan, B. Watts, L. N. Jan, C. R. McNeill, H. Ade, *Nano Lett.* **2010**, *10*, 2863; b) J. R. Tumbleston, B. A. Collins, L. Q. Yang, A. C. Stuart, E. Gann, W. Ma, W. You, H. Ade, *Nat. Photonics* **2014**, *8*, 385; c) B. A. Collins, J. E. Cochran, H. Yan, E. Gann, C. Hub, R. Fink, C. Wang, T. Schuettfort, C. R. McNeill, M. L. Chabinyc, H. Ade, *Nat. Mater.* **2012**, *11*, 536; d) L. Ye, S. Q. Zhang, W. Ma, B. H. Fan, X. Guo, Y. Huang, H. Ade, J. H. Hou, *Adv. Mater.* **2012**, *24*, 6335.

[23] T. Coffey, S. G. Urquhart, H. Ade, *J. Electron Spectrosc.* **2002**, *122*, 65.

[24] a) B. A. Collins, Z. Li, J. R. Tumbleston, E. Gann, C. R. McNeill, H. Ade, *Adv. Energy Mater.* **2013**, *3*, 65; b) J. J. van Franeker, M. Turbiez, W. Li, M. M. Wienk, R. A. Janssen, *Nat. Commun.* **2015**, *6*, 6229.

[25] a) W. Chen, T. Xu, F. He, W. Wang, C. Wang, J. Strzalka, Y. Liu, J. G. Wen, D. J. Miller, J. H. Chen, K. L. Hong, L. P. Yu, S. B. Darling, *Nano Lett.* **2011**, *11*, 3707; b) H. Y. Lu, B. Akgun, T. P. Russell, *Adv. Energy Mater.* **2011**, *1*, 870; c) Y. Gu, C. Wang, T. P. Russell, *Adv. Energy Mater.* **2012**, *2*, 683; d) F. Liu, Y. Gu, C. Wang, W. Zhao, D. Chen, A. L. Briseno, T. P. Russell, *Adv. Mater.* **2012**, *24*, 3947; e) M. J. Zhang, X. Guo, W. Ma, S. Q. Zhang, L. J. Huo, H. Ade, J. H. Hou, *Adv. Mater.* **2014**, *26*, 2089.

[26] E. Gann, A. T. Young, B. A. Collins, H. Yan, J. Nasiatka, H. A. Padmore, H. Ade, A. Hexemer, C. Wang, *Rev. Sci. Instrum.* **2012**, *83*, 045110.

[27] A. Hexemer, W. Bras, J. Glossinger, E. Schaible, E. Gann, R. Kirian, A. MacDowell, M. Church, B. Rude, H. Padmore, *J. Phys. Conf. Ser.* **2010**, *247*, 012007.

Adv. Mater. **2015**,
DOI: 10.1002/adma.201502110